Individual Tree-Crown Delineation and Treetop Detection in High-Spatial-Resolution Aerial Imagery

Le Wang, Peng Gong, and Gregory S. Biging

Abstract

The cost of forest sampling can be reduced substantially by the ability to estimate forest and tree parameters directly from aerial photographs. However, in order to do so it is necessary to be able to accurately identify individual treetops and then to define the region in the vicinity of the treetop that encompasses the crown extent. These two steps commonly have been treated independently.

In this paper, we derive individual tree-crown boundaries and treetop locations under a unified framework. We applied a two-stage approach with edge detection followed by marker-controlled watershed segmentation. A Laplacian of Gaussian edge detection method at the smallest effective scale was employed to mask out the background. An eight-connectivity scheme was used to label the remaining tree objects in the edge map. Subsequently, treetops are modeled based on both radiometry and geometry. More specifically, treetops are assumed to be represented by local radiation maxima and also to be located near the center of the tree-crown. As a result, a marker image was created from the derived treetop to guide a watershed segmentation to further differentiate touching and clumping trees and to produce a segmented image comprised of individual tree crowns.

Our methods were developed on a 256- by 256-pixel CASI image of a commercially thinned trial forest. A promising agreement between our automatic methods and manual delineation results was achieved in counting the number of trees as well as in delineating tree crowns.

Introduction

Modern forest management requires that forest resources be efficiently managed, not only for timber production, but also for such purposes as maintaining biodiversity and meeting wildlife, environmental, and recreational needs. Accordingly, there is an increasing need for detailed knowledge of forest stands, which are the basic units for forest management. Inevitably, stand measurement involves the measurement of individual trees within the stand. The traditional method for deriving stand information is to utilize sampling designs with transects, random or systematically selected plots, so that the final stand parameters can be derived based on statistical extrapolation methods. By utilizing remote sensing data, we can reduce the amount of field sampling; hence, information gathering becomes more cost-effective.

In the 1940s, manual interpretation of medium- and large-scale aerial imagery for forestry emerged (Brandtberg, 1999). Since then, field inventory in combination with aerial photointerpretation has played an important role in forest data collection. The visual aerial photointerpretation method is labor-intensive, time-consuming, and dependent on the interpreter's experience. Thus, there is merit for developing an automated or semiautomated aerial photo measurement method for forest trees.

With the increasing availability of large-scale and high-resolution imagery, a new round of research on computer-based photointerpretation of trees was recently initiated (Gong *et al.*, 1999). Various algorithms have been developed for automatic individual tree recognition. They can be grouped into four major types: local maximum (LM)-based methods (Blazquez, 1989; Dralle and Rudemo, 1996), contour-based (CB) methods (Pinz *et al.*, 1993; Gougeon, 1995), template-matching (TM)-based methods (Pollock, 1996; Tarp-Johansen, 2002), and 3D-model-based methods (Sheng *et al.*, 2001; Gong *et al.*, 2002).

The LM method makes the assumption that the peak of the tree-crown reflectance is located at or very close to the treetop (Brandtberg and Walter, 1998). Therefore, by filtering the image to find the local maximum, treetops are finally detected. An image-smoothing step can be introduced in this method to reduce the noise effect (Dralle and Rudemo, 1996). In addition, LM methods can be combined with an advanced region-based analysis of the image objects (Pinz *et al.*, 1993). Although this method has the merit of being fast and simple, it performs poorly when undesirable background phenomena and varying illumination conditions exist in the image.

The TM method includes a model generation and a template-matching procedure (Pollock, 1996). Intuitively, a series of models are built to characterize what a tree looks like at different locations in an image by taking into consideration both the trees' geometric and radiometric properties. Once this knowledge is gained, a moving-window correlation procedure is implemented to search for the locus of best matching where trees are most likely to be.

From another perspective, the CB method attempts to find the delimiter between tree crowns and their background. Briefly, the main strategy here is either to follow the intensity valleys underlying the image (Gougeon, 1995) or to detect the crown boundary with edge-detection methods (Brandtberg and Walter, 1998). For the valley-following method, a set of rules is predefined before the actual crown following takes place. Few people endeavor to use the edge-detection method

Center for Assessment and Monitoring of Forest and Environmental Resources (CAMFER), 145 Mulford Hall, University of California, Berkeley, CA 94720-3114 (gong@nature.berkeley.edu)

Photogrammetric Engineering & Remote Sensing
Vol. 70, No. 3, March 2004, pp. 351–357.

0099-1112/04/7003–0351/$3.00/0

because of two major difficulties. First, intensity changes can occur over a wide range of scales. For example, at finer scales all branches in a tree-crown image are visible. Thus branches account for most of the changes in intensity. At a coarser scale, a tree crown may merge with its neighbors (Brandtberg and Walter, 1998). Therefore, groups (clusters) of trees might be where the changes occur. As a result, to find the right scale that corresponds exactly to individual tree-crown boundaries is difficult. Sometimes, given the complex reflectance situation in a forested area, it may be impossible to find a scale that is applicable for all individual trees of the same image. Second, edge detection is a low-level image processing procedure, which can only provide raw primal sketches. Individual tree-crown delineation is a high-level vision problem that requires expert knowledge. Therefore, additional steps are needed to improve edge-detection algorithms to make use of biological knowledge concerning tree-crown shapes. In this way we can fill the apparent gaps between edge detection and tree-crown delineation.

3D-based methods have been applied by fewer researchers in comparison to other types of methods. Sheng *et al.* (2001) employed model-based image matching to obtain an improved tree-crown surface reconstruction. They utilized a parametric tree-crown surface model that takes into consideration crown shape, illumination, and a sensor model. As a further improvement, Gong *et al.* (2002) developed an interactive tree interpreter to generate the tree model providing the means for semiautomatic tree-crown segmentation. To fully automate this method, however, a necessary step is to automatically determine the treetop locations separately on the left and right epipolar images.

This paper has two major objectives: (1) to incorporate geometry and radiometry in the process of locating treetops and (2) to develop and test a two-stage tree-identification method (edge detection followed by marker controlled watershed segmentation). It is hoped that, as a result of this two-stage process, treetops can be more accurately located and that these locations will assist in the process of delineating tree-crown boundaries.

Study Site and Data Preparation

Study Site

Our study area is centered at N53° 59′, W122° 10′, which is approximately 40 km northeast of Prince George, British Columbia, Canada, and is approximately 8 hectares in size. The mean elevation of the study area is approximately 715 meters. The terrain consists of a relatively flat (relief less than 3 m) bench of glacial deposits. The forest at the study site is part of a commercial thinning trial that was established in 1986. It is comprised of 80-year-old fire origin white spruce trees (*Picea glauca*) with a minor portion of interior Douglas fir (*Pseudotsuga menziesii* (Mirb.) Franco) and subalpine fir (*Abies lasiocarpa*). The density is 650 live stems/ha. The entire stand is relatively uniform with respect to topography, ecosystem unit, stocking, and disease incidence and extent (Reich and Price, 1998).

Data Preparation

A 512- by 512-pixel CASI (Compact Airborne Spectrographic Imager) image was collected on 07 October 1996 under conditions of uniform cloud cover by Itres Research Ltd. CASI has two operating modes: spectral and spatial. However, only the spatial mode was employed in this study. The nominal spatial resolution of the image is 0.6 m and the nominal flying height is 375 m above ground. The field of view is approximately 45°. Spectral data were collected in eight bands, whose wavelengths are as follows: two blue (450 and 500 nm), green (550 nm), orange (600 nm), red (650 nm), red edge (715 nm), and two near-infrared (780 and 840 nm). The image was radiometrically and geometrically corrected to a uniform elevation without the use of a digital terrain model (Reich and Price, 1998).[1] Only the center portion of the original image (256 by 256 pixels, 2.36 ha) was selected for use in this study in order to maintain a near-nadir perspective across the subimage to be analyzed (Figure 1).

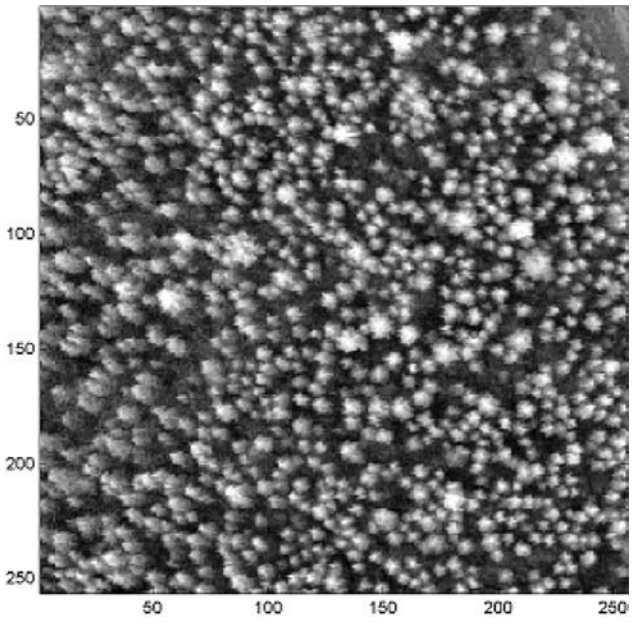

Figure 1. First PCA component image of the study area.

Methods

A systematic framework of our algorithm is presented in Figure 2. The algorithm can be divided into two stages. The first stage utilizes an edge-detection method to obtain initial tree-crown boundaries. The second stage can be separated into two main parts: treetop marker selection and marker-controlled watershed segmentation. The following sections describe each step in detail.

Edge Detection

Tree crown, understory vegetation, and bare soil comprise the major portion of the forest image. This gives rise to the first step, which is to separate trees from their background. Multispectral images provide more information for use in the separation procedure and in some sense can help compensate for coarse spatial resolution (Pollock, 1996). However, current edge-detection methods can be applied only to a single-band image. Therefore, we used Principal Components Analysis (PCA) to obtain a suitable single-band image for our study. PCA transforms a set of images into a new set of images (components) with as little correlation between components as possible. The first component contains the most variance, and each subsequent component contains less variance than the previous component (Ricotta *et al.*, 1999). Therefore, we selected the first principal component as our single-band image for edge-detection processing.

[1]Because the maximum elevation change is 3 m for this forest area, radiometric and geometric correction to a uniform elevation involves minimal error.

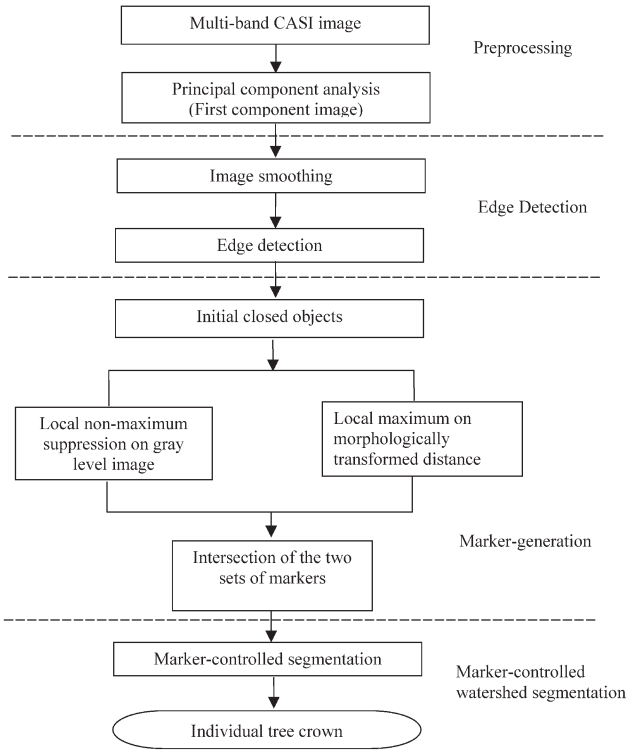

Figure 2. Diagram of the procedures used in the study.

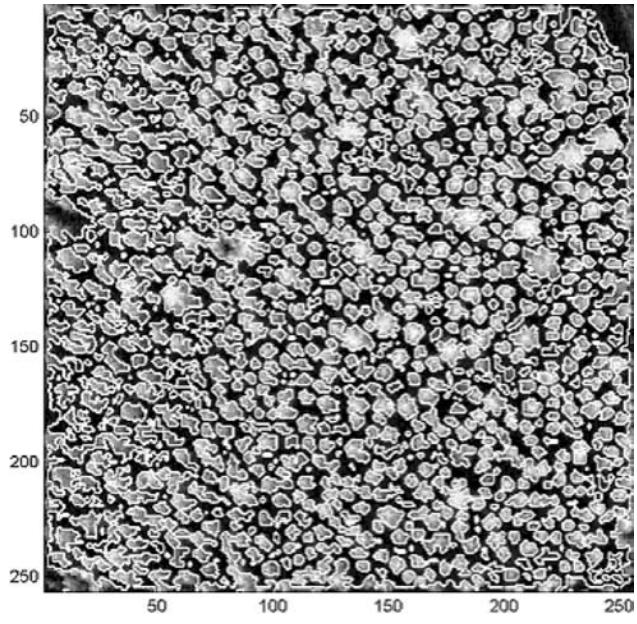

Figure 3. Resultant image after LOG edge detection ($\sigma = 1$).

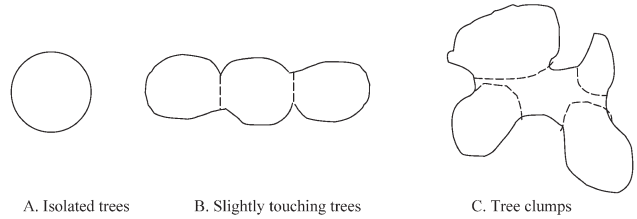

Figure 4. Three typical cases of objects after smoothing and edge detection. (a) Isolated trees. (b) Slightly touching trees. (c) Tree clumps.

An edge in an image corresponds to an intensity discontinuity of the underlying scene. This intensity discontinuity may arise from a depth discontinuity, a surface normal discontinuity, a reflectance discontinuity, or an illumination discontinuity (Marr and Hildreth, 1980). Edge continuities in a forest at high latitudes are caused by the contrast of tree crowns and background, and the illumination discontinuity is caused by shadow. Edge-detection methods can be used to derive the initial boundary of the tree crown. This allows us to mask out non-tree areas and retain tree-crown objects for further segmentation and analysis.

We chose Laplacian of the Gaussian (LOG) operator as our edge-detection method. The LOG method can be divided into two steps. At the first step, a Gaussian smoothing (convolution) is applied to the image to remove noise as well as intensity variation due to the tree's internal structure. A second step is to find the zero of the second derivative of the smoothed image. The LOG detector is written as (Marr, 1980)

$$LoG(x, y) = -\frac{1}{\pi\sigma^4}\left[1 - \frac{x^2 + y^2}{2\sigma^2}\right]\exp\left(-\frac{x^2 + y^2}{2\sigma^2}\right).$$

The smoothing scale σ in pixels determines the minimum width of the edge that can be captured. Although it may be useful to implement the LOG operator at a series of scales, it is very difficult to integrate the outputs from multiple scales (Lu and Jain, 1989). Therefore, we chose a single smoothing scale of one pixel ($\sigma = 1$), which represents the smallest tree-crown diameter (0.6 m by visual inspection) in the image. The LOG detector can also produce artifacts that are referred to as phantom edges, and so it is necessary to distinguish these phantom edges from authentic edges. We used a method proposed by Clark (1989) to retain only authentic edges for subsequent higher-level vision processing (Figure 3).

In the final edge-detection step the dark background was masked out and the remaining edge pixels were labeled using an eight-connectivity scheme to generate a series of closed contours. However, to obtain the final individual tree crowns, further segmentation of these contours is needed. Generally, there exist three typical cases for the closed contours obtained by the method we applied (Brandtberg, 1999) (Figure 4). Isolated single trees have, at some appropriate scale level, a single circular shaped contour, while slightly touching trees and clumped trees may have irregular or oblong shapes. We dealt with these different cases by first identifying treetops within each contour, and then using the treetops as guides for determining the final tree crowns.

Marker Generation

Each closed contour derived by edge detection is treated as one object, and for each object we determine how many trees it contains by locating and labeling treetops. Treetops have their own unique radiometric and spatial characteristics. Under normal conditions the radiation intensity measured from an individual tree varies and is highest on the uppermost sunlit portion of the tree crown. Thus, we use a local non-maximum suppression method to obtain one set of treetops. Spatially, a treetop is located at or near the center of the tree

crown when it is viewed from a near-nadir perspective. Thus, we use a local maximum-distance method to obtain another set of treetops. A treetop that is identified by both methods is labeled as a marker.

Local Non-Maximum Suppression on Gray Level Image
The purpose of using the local non-maximum suppression method is to create a binary image in which each treetop is represented by one pixel with a value of one, and all other pixels with a value of zero. This is accomplished by using a sliding window that assigns a value of one to the center pixel if all surrounding pixel values within the window are less than the value of the center pixel. This method has been proven (Dralle and Rudemo, 1996), under some restrictions, to be effective in locating treetops, and so we applied it to each crown object individually, using the gray values from the first component PCA image that we used for edge detection. The proper window size is critical for this method to succeed. If the window size is too small, some trees with large crown radii are assigned more than one treetop. Conversely, if the window size is too large, trees with crown radii shorter than the specified radius are not assigned a treetop. In this study we chose a comparatively small radius (3 by 3 window) to ensure that small isolated trees were not missed. Any false treetops that may be identified were eventually filtered out by the results of the following spatial algorithm.

Local Maximum on Morphologically Transformed Distance
A second consideration for the selection of markers is based on a spatial perspective. At or near nadir view, treetops are usually located around centers of tree crowns. To utilize this knowledge in searching for treetops, we used a geodesic distance transformation, which is a concept borrowed from mathematical morphology. The geodesic distance between two pixels p and q in set A is defined as the length of the shortest path joining p and q within A. In the same manner, the geodesic distance from any pixel in set A to its complement set is defined as the distance of that pixel in A to the nearest pixel in the complement of A. The distance between two pixels is calculated based on the properties of a structure element (SE), which is a group of connected pixels that resembles the geometry of the object to be measured. Distance can be measured only along connected paths as defined by the SE, and the length of each step is determined by the value of each pixel in the SE. An SE is usually built as a small window of pixels with either one or zero as pixel values (Soille, 1999).

Based on the assumption that treetops are located in the vicinity of the center of the tree crown, an elementary disk SE (3 by 3 window of pixels whose values are all equal to 1) was adopted to calculate geodesic distance. This elementary disk SE allows the calculation of geodesic distance with eight-connected neighborhoods as opposed to using an elementary cross SE with four-connected neighborhoods. For each object derived and labeled in the edge-detection step, we created a binary mask with the object interior represented by a value of one, and the exterior represented by a value of zero. The geodesic distance between each interior pixel and the set of exterior pixels was calculated, and a resultant distance image of the object was formed with the exterior pixels having values of zero. As defined above, the value of a pixel in the distance image can be interpreted as the geodesic distance from that interior pixel to the nearest exterior pixel. Subsequently, for each object we extract the regional maximum of the distance image. Here, the regional maximum is defined as a connected group of pixels with a single distance value such that each pixel in the group has a value greater than or equal to all the pixel values within the surrounding eight-connectivity neighborhood. As a result of the extraction, the regional maximum is usually found near the center of the object, and thus the regional maximum is labeled as a treetop.

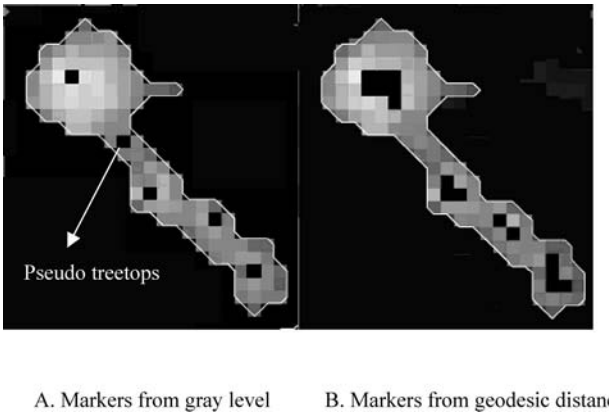

Figure 5. An example of markers filtering process. (a) Markers from gray level. (b) Markers from geodesic distance.

Marker Image Generation by Intersection of the Two Sets of Treetops
In order to satisfy the two assumptions associated with treetops and set the final markers, we intersected the two sets of candidate treetops that were obtained by the procedures previously described. To accomplish this, each treetop obtained from gray-level non-maximum suppression was tested for proximity to a treetop identified by the maximum-distance method. If a maximum-distance treetop is located within a 3 by 3 window surrounding a gray-level treetop, then this treetop is selected as a final treetop marker. This intersection process is performed on each crown object separately. Figure 5 illustrates how this method filters out false treetops. There are five candidate treetops resulting from the non-maximum suppression of the gray-level image, but there are only four based on maximum local distance. The four coinciding treetops become the final treetop markers, while the fifth treetop is rejected as a pseudo treetop. In this study, 1536 candidate treetops were found by the non-maximum suppression method in the beginning. After intersection with the set of maximum-distance candidate treetops, a total of 1240 treetops was retained. The final marker set was stored as a treetop marker image with marker pixel values equal to one and the rest of the pixel values equal to zero (Figure 6). These treetop markers then served as guides for the watershed segmentation so that all the individual tree crowns could be delineated.

Marker-Controlled Watershed Segmentation

Traditionally, marker selection and marker-controlled watershed segmentation is applied to the whole image at one time. This can introduce error due to interference from the background. In the prior section we determined the final treetop markers by integrating the results from gray-scale and morphological analysis of individual crown objects. The only remaining task is to delineate the tree-crown boundary for each individual tree within each crown object. This segmentation task is also performed on individual objects, rather than on the entire image. In this way we eliminate the error that would otherwise be introduced by the background.

Geometric information is valuable for segmenting individual trees in high-spatial-resolution imagery. The field of mathematical morphology contains a whole set of nonlinear image processing and analysis methods which focus on exploring the geometric structure in an image (Soille, 1999). The advantages of these nonlinear methods are their ability to selectively preserve structural information while accomplishing

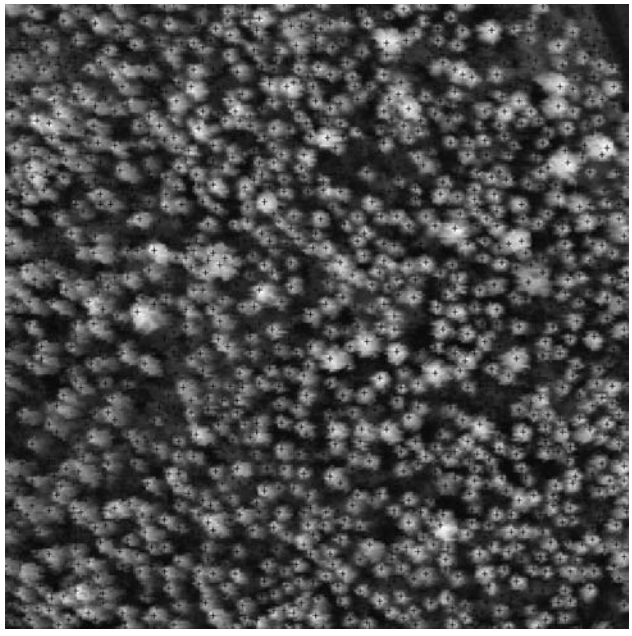

Figure 6. Marker image by intersecting the two sets of treetops.

desired tasks on the image. Watershed segmentation belongs to this family of methods, which was first introduced by Beucher and Lantuejoul and later defined mathematically by both Meyer and others (Pesaresi and Benediktsson, 2001). A further variant of this method is so called "marker[2]-controlled watershed segmentation." Intuitively, this method can be understood as in the following. A gray-scale image can be treated as a topographic model. The gray tone of each pixel stands for the elevation at that point (Vincent and Soille, 1991). If we invert the gray tone for each point, the local gray-tone maxima on the original image becomes the local minima, which lie in valleys. If water is introduced to the system, each valley will collect water, starting at the marker (local minimum), until the water spills over the watershed into an adjacent valley. The watersheds that surround the valleys constitute closed contours, which separate the whole area into different catchment basins, each containing a marker (local minimum). As a result, these closed contours are the desired boundaries of each object.

The success of the above segmentation method relies on correct marker selection. Due to the presence of spurious local minima and maxima, traditional marker-controlled watershed segmentation often results in severe over-segmentation (Soille, 1999). As described earlier, we have addressed this problem by obtaining an accurate treetop marker set.

Another factor affecting the success of segmentation is the correlation between the gray-level image patterns and the desired object boundaries. Therefore, for each object, we chose to create images that represent the geodesic distances from each interior pixel to each treetop marker. This process of determining the boundary is also known as the formation of geodesic skeleton by use of influence zones (Soille, 1999). First, the geodesic distance from each pixel to each marker is calculated according to the elementary disk SE as described earlier. Next, for a specified marker K_i, its influence zone is the locus of points whose geodesic distance to K_i is smaller than their geodesic distance to any other markers. Once the influence zone of each marker is determined, the boundaries between these influence zones represent the desired crown boundaries. The next step is to generate the crown boundary (watershed) line around each treetop marker. The final step is reassembling all the individual tree crowns back into a whole image. We listed in Table 1 the various window sizes and SE parameters used in our methods.

[2]A marker is an image feature (connected pixels of constant reflectance values, areas of uniform texture, or in our case treetops) useful in identifying different objects.

TABLE 1. PARAMETERS USED IN OUR METHODS

Parameters	Values Assigned (pixel)
σ assigned in the LOG	1
Window size of non-maximum suppression	3 by 3
SE used to calculate regional maximum of geodesic distance	3 by 3 window with all values equal to one
Window size of the treetop intersection	3 by 3

Experimental Results

Experimental Results

Our algorithm was implemented in Matlab 5.3 for the selected 256 by 256 subimage. A total of 1240 trees were detected, and their corresponding tree crowns were delineated by the methods given earlier. To present our results, we manually divided the original image into three portions according to their relative directions to the nadir: left-side portion, center portion, and right-side portion. Figure 7 provides the separate results for each portion. Trees at the image border posed a special problem in that their crowns were not always fully contained in the image and, hence, we could not utilize morphological analysis for delineating these tree crowns. Therefore, we did not include border trees in our analysis. This resulted in the removal of 118 trees, and a reduction in the coverage area to

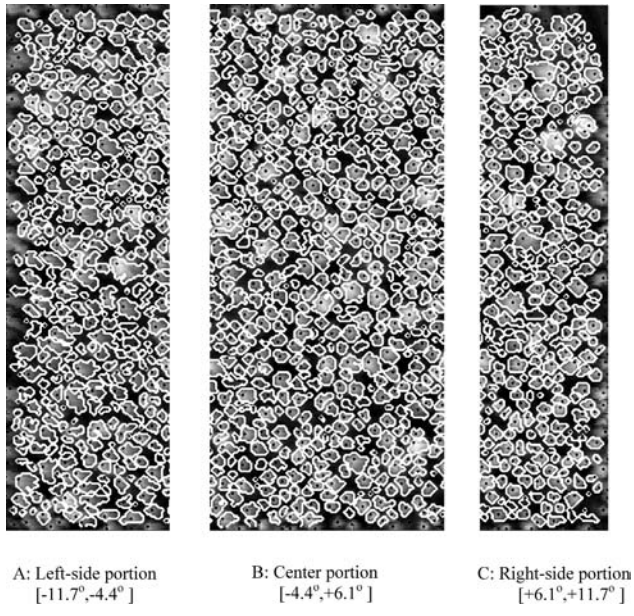

Figure 7. Computer delineated tree crowns and identified treetops for three different portions. (a) Left-side portion (−11.7° to −4.4°). (b) Center portion (−4.4° to +6.1°). (c) Right-side portion (+6.1° to +11.7°).

1.86 ha. The remaining 1122 trees were fully contained within the image and were the ones used in subsequent analysis.

Results Evaluation

We do not have a surveyed tree crown map to use as our reference data, but we do know that the average tree density is 650 trees/ha. While there is some variation in density throughout the study area, it does not vary greatly from the average because the study area is a managed forest. Therefore, we estimate that there are 1211 trees (1.86 ha by 650 trees/ha). However, this estimated number could only be used as a general guide for the number of trees in this study.

To evaluate our algorithm, we conducted a visual interpretation based on the standard false-color composite of the original image. Three graduate students with strong forestry backgrounds spent four hours each delineating tree crowns on a computer screen. They were asked to not count trees that were partially off of the image. These students identified 954, 975, and 942 stems, respectively. Because their results were quite similar for both the number of trees and tree-crown locations, we averaged their results and generated a comparatively reliable reference dataset. The average number of trees found by manual delineation was 957, or 85.3 percent of the 1122 trees automatically determined by our algorithm. A visual inspection showed that the difference in number of trees between the manual and automatic results is mostly due to the difficulty in visually identifying small trees (isolated individuals and in clumps). In addition, we superimposed the automatically delineated contours onto the false-color composite image so that we could determine if there were specific conditions associated with misclassification. It appeared that misclassification was primarily associated with large, circular-shaped clumps in the image. In these cases, it was difficult to tell visually whether there were several smaller tree crowns aggregated together or if there was only one large tree instead. This overlay also showed that the manual operators missed many small, isolated trees.

To further investigate the performance of tree-crown delineation, we overlaid the automatically detected tree-crown image with one of the manually delineated crown images. We found a high correspondence between the two images with regard to the delineated crown areas. Strict comparison shows that 75.6 percent of the total pixels are classified identically (crown or non-crown) in both images (Table 2). The actual classification overlap, however, would be higher than 75.6 percent if the clumped trees were properly identified by manual delineation. This is because fewer crown pixels would be identified manually in the clumps, which is in better agreement with the multiple trees found by the automated process. The percentage would also rise if more of the isolated small trees were also identified by manual delineation. This shows that our algorithm detected most of the visually interpreted tree crowns as well as detecting some trees that were missed by visual interpretation.

TABLE 2. AGREEMENTS OF THE DETECTED CROWN CLOSURE BETWEEN THE MANUAL AND AUTOMATIC METHODS

		Manual delineation (pixels)		
		Tree crown	Non-tree area	Total
Automatic Delineation (pixels)	Tree crown	15055	12041	27096
	Non-tree area	3972	34468	38440
Total		19027	46509	65536
Average agreement: 75.6%				

A visual comparison of the three results derived for different portions of the original image (Figure 7) shows that our algorithm performed best in the center portion, as expected. For the other two slightly off-center portions, our algorithm still can capture most tree-crown boundaries although some misclassification occurred on large tree clumps.

Discussion

Treetop detection and tree-crown delineation have previously been treated as two separate procedures by most researchers. However, due to the close relationship between treetop and tree-crown boundaries, they should be considered together so that the derivation of one part can assist in the solution of another. In our algorithm, treetop detection utilizes both radiometric and geometric information from tree crowns. The derived treetop serves as a marker to control the watershed segmentation, which finally allows us to derive individual tree-crown boundaries. Therefore, both treetop and individual tree-crown boundaries are products of our algorithm.

As noted above, shape information plays an important role in individual tree-crown delineation. However, existing algorithms have not effectively exploited such morphological information. In our methods, with the aid of local maximum of geodesic distance, we actually superimposed a geometric restriction on traditional radiometric non-maximum suppression methods to derive treetop markers. The satisfaction of two assumptions, one based on geometry and one based on radiometry, largely reduces the error introduced during the non-maximum suppression treetop selection step. By using treetops as the markers, we have effectively adapted the original watershed segmentation to the tree-crown delineation problem.

Although our algorithm takes advantage of both spectral and spatial information in order to separate individual trees and to locate treetops, there still exist some potential problems deserving further research:

- *Limitation of the Assumptions*. The assumption that treetops are located around the vicinity of the center of a crown can be met only when the view area is within $\pm 15°$ of nadir. This assumption may not be applicable to trees located outside of this range because treetops lean away from the nadir point. Our current algorithm can be improved by including different treetop models that are based on the location of trees. The view angle of CASI is 45°, and our test image was selected at the middle of a 512- by 512-pixel image, thus keeping the edges of our test image within 11.7 degrees of nadir. This means that our method is effective within this range.
- *Scale Effects*. Because trees are of different sizes, a multi-scale strategy should be eventually adopted. The σ value in the LOG edge detection, the window size of non-maximum suppression, the window size of the treetop intersection method, and the SE used in the mathematical morphology were all assigned a fixed value based on the minimum tree-crown size. However, these parameters could be varied, and the intermediate results obtained from different scales could be integrated to obtain the final results.
- *Tree-Crown Boundaries Are Sometimes Inconsistent with Gray-Scale Boundaries*. For trees viewed from the near-nadir direction, crown boundaries can be well matched with the gray-scale edges recorded in the digital images. However, for trees viewed from outside the near-nadir direction, the silhouettes detected from edge-detection methods are inconsistent with the real tree-crown boundaries. This problem might be overcome by using 3D-based methods.

Conclusions

Treetops have their own radiometric and spatial characteristics. Many researchers have intensively explored the radiometric characteristics of tree crowns. However, it is hard to define an appropriate window size to capture the real treetops

while filtering out the false ones. On the other hand, spatial characteristics are valuable in locating treetops, but they have rarely been applied due to the difficulty of expressing shape information in discrete image space. With the aid of mathematical morphology, we developed a way to integrate spatial information with a radiometric method by extracting the regional maximum of geodesic distance. The combined use of radiometry and geometry in this study effectively captured the majority of treetops, and also largely reduced the occurrence of pseudo ones.

Tree crowns and treetops are closely related parameters, and thus we believe they should be solved for together. Marker-controlled watershed segmentation provides a solid base to combine treetop detection and tree-crown delineation under a unified framework. By defining the treetops as markers and using them to guide the watershed line generation, we developed a strategy to accomplish treetop detection and tree-crown delineation simultaneously. Our initial results indicate that edge detection may be quite useful in differentiating trees from non-tree areas. Marker-controlled segmentation, when based on a good estimation of treetop markers, may solve the problems of slightly touching trees and clumped trees. The results of our proposed treetop detection and individual tree-crown delineation algorithm achieved promising agreements with the results from manual delineation, but our algorithm needs to be more fully tested with independent ground reference data.

Acknowledgments

The authors would like to acknowledge the CASI image provided by the ITRES, Ltd Canada; Manual interpretation by Xia Gong, Qian Yu, and DeSheng Liu; and helpful suggestions by Alan Di Vittorio.

References

Blazquez, C.H., 1989. Computer-based image analysis and tree counting with aerial color infrared photography, *Journal of Imaging Technology*, 15(4):163–168.

Brandtberg, T., 1999. *Remote Sensing for Forestry Applications—A Historical Retrospect*, http://www.dai.ed.ac.uk/CVonline/LOCAL_COPIES/BRANDTBERG/UK.html (last accessed 13 October 2003).

Brandtberg, T., and F. Walter, 1998. Automated delineation of individual tree crowns in high spatial resolution aerial images by multiple-scale analysis, *Machine Vision and Applications*, 11(2):64–73.

Dralle, K., and M. Rudemo, 1996. Stem number estimation by kernel smoothing of aerial photos, *Canadian Journal of Forest Research-Revue Canadienne De Recherche Forestiere*, 26(7):1228–1236.

Gong, P., G.S. Biging, S.M. Lee, X. Mei, Y. Sheng, R. Pu, B. Xu, K.P. Schwarz, and M. Mostafa, 1999. Photo-ecometrics for forest inventory, *Geographic Information Sciences*, 5(1):9–14.

Gong, P., Y. Sheng, and G.S. Biging, 2002. 3d model-based tree measurement from high-resolution aerial imagery, *Photogrammetric Engineering & Remote Sensing*, 68(11):1203–1212.

Gougeon, F.A., 1995. A crown-following approach to the automatic delineation of individual tree crown in high spatial resolution aerial images, *Canadian Journal of Remote Sensing*, 21(3): 274–284.

Lu, Y., and R.C. Jain, 1989. Behavior of edges in scale space, *IEEE Transactions on Pattern Analysis and Machine Intelligence*, 11(4):337–356.

Marr, D., and E. Hildreth, 1980. Theory of edge-detection, *Proceedings of the Royal Society of London Series B-Biological Sciences*, 207(1167):187–217.

Pesaresi, M., and J.A. Benediktsson, 2001. A new approach for the morphological segmentation of high-resolution satellite imagery, *IEEE Transactions on Geoscience and Remote Sensing*, 39(2):309–320.

Pinz, A., M.B. Zaremba, H. Bischof, F.A. Gougeon, and M. Locas, 1993. Neuromorphic methods for recognition of compact image objects, *Machine Graphics and Vision*, 2(3):209–229.

Pollock, R., 1996. *The Automatic Recognition of Individual Trees in Aerial Images of Forests Based on a Synthetic Tree Crown Image Model*, Ph.D. Thesis, University of British Columbia, Vancouver, Canada, 158 p.

Reich, R., and R. Price, 1998. Detection and classification of forest damage caused by tomentosus root rot using an airborne multispectral imager (Casi), *Proceedings of International Forum: Automated Interpretation of High Spatial Resolution Digital Imagery for Forestry*, 10–12 February, Victoria, B.C., Canada (Canadian Forest Service), pp. 179–186.

Ricotta, C., G.C. Avena, and F. Volpe, 1999. The influence of principal component analysis on the spatial structure of a multispectral dataset, *International Journal of Remote Sensing*, 20(17): 3367–3376.

Sheng, Y.W., P. Gong, and G.S. Biging, 2001. Model-based conifer-crown surface reconstruction from high-resolution aerial images, *Photogrammetric Engineering & Remote Sensing*, 67(8):957–965.

Soille, P., 1999. *Morphological Image Analysis: Principles and Applications*, Springer, Berlin: New York, 319 p.

Tarp-Johansen, M.J., 2002. Automatic stem mapping in three dimensions by template matching from aerial photographs, *Scandinavian Journal of Forest Research*, 17(4):359–368.

Vincent, L., and P. Soille, 1991. Watersheds in digital spaces—An efficient algorithm based on immersion simulations, *IEEE Transactions on Pattern Analysis and Machine Intelligence*, 13(6):583–598.

(Received 14 November 2001; revised and accepted 01 April 2003)